OPEN ACCESS
International Journal of Innovations in Science & Technology

Investigating The Impact of Perovskite Layer Thickness Variation on The Performance of Perovskite Solar Cells

Amna Khan, Muhammad Nasir, Muhammad Yasir Jamal, Muhammad Shahid, Muhammad Danish Nisar, Aashir Waleed*

Department of Electrical Electronics and Telecommunication Engineering, University of Engineering & Technology, Lahore (Faisalabad), Pakistan

***Correspondence**: aashir.walid@uet.edu.pk

Citation | Khan. A, Nasir. M, Jamal. M. Y, Shahid. M, Nisar. M. D, Waleed. A, "Investigating the Impact of Perovskite Layer Thickness Variation on The Performance of Perovskite Solar Cells", IJIST, Vol. 07 Issue. 02 pp 1120-1131, May 2025

Received| April 07, 2025 **Revised|** May 29, 2025 **Accepted|** June 02, 2025 **Published|** June 04, 2025.

The present risk of the depletion of the non-renewable sources of energy at an alarming rate has encouraged man to look for new ways to produce power and move towards "Renewable Energy Resources". One major source of energy is the heat and intensity from the Sunlight using the Perovskite Solar Cells. This technology has captured extensive attention worldwide in the previous few years due to its high efficiency, fast development, low cost, and easy manufacturing process. In this research, the thickness variation of different types of perovskite layers and their impacts on the functioning of the perovskite solar cells have been explored using SCAPS software. The absorption coefficient of semiconducting material is exponentially related to the thickness, so if the absorption coefficient is high, the lesser thickness can absorb more light. But to avoid excessive resistance and to lessen the production cost, the thickness should be in the range of the depletion region width. Much smaller thickness yields weak static electric fields in the depletion region. The designs of different perovskite solar cell structures will be simulated and their effects will be critically analyzed in order to have a detailed study.

Keywords: Solar Cells, Perovskite, Energy, Irradiation, SCAPS

Introduction:

Optoelectronic devices operate based on the principle of converting optical energy into electrical energy [1]. A solar cell is a common example of such a device. Semiconducting materials are used to manufacture optoelectronic devices because of a number of advantages such as stable device performance, variety of semiconducting materials, light detection from a broad spectrum (ultraviolet to infrared) owing to the huge variety of different band gaps and compatibility with lithography process helps in device miniaturization and integration.

There has been a surge of attention in organic and inorganic metallic halide-based perovskites in the past few years due to their remarkable properties. These metal halide perovskite materials show great potential for use in excellent-performing optoelectronic devices, thanks to their outstanding electrical and optical characteristics. Electrical and optical qualities include exceptional optical absorption, high carrier mobility, great efficiency in converting solar energy, impressive luminescence efficiency, and long carrier diffusion length. As a result, these materials have become a prime area of research and development, with scientists and engineers working tirelessly to unlock even more exciting possibilities for their future applications [2][3][4][5][6].

Perovskite materials offer vast opportunities for next-generation high-performance solar cells, photodetectors, and LEDs across a wide range of applications including energy conservation and communication. With their attractive compositional tunability and unique physical properties, these materials have unlocked a plethora of possibilities for researchers and developers alike. Best of all, they allow for the creation of novel materials with distinct characteristics, paving the way for even more exciting discoveries in the future.

Over the years, numerous photovoltaic (PV) materials have been discovered and utilized in solar cell fabrication. Figure 1 provides an overview of these materials, highlighting the periods during which they reached their peak energy conversion efficiencies. Efficiency timeline can be visualized from Figure 1 which indicates that perovskite materials have shown remarkable increment in their efficiency in a very short time.

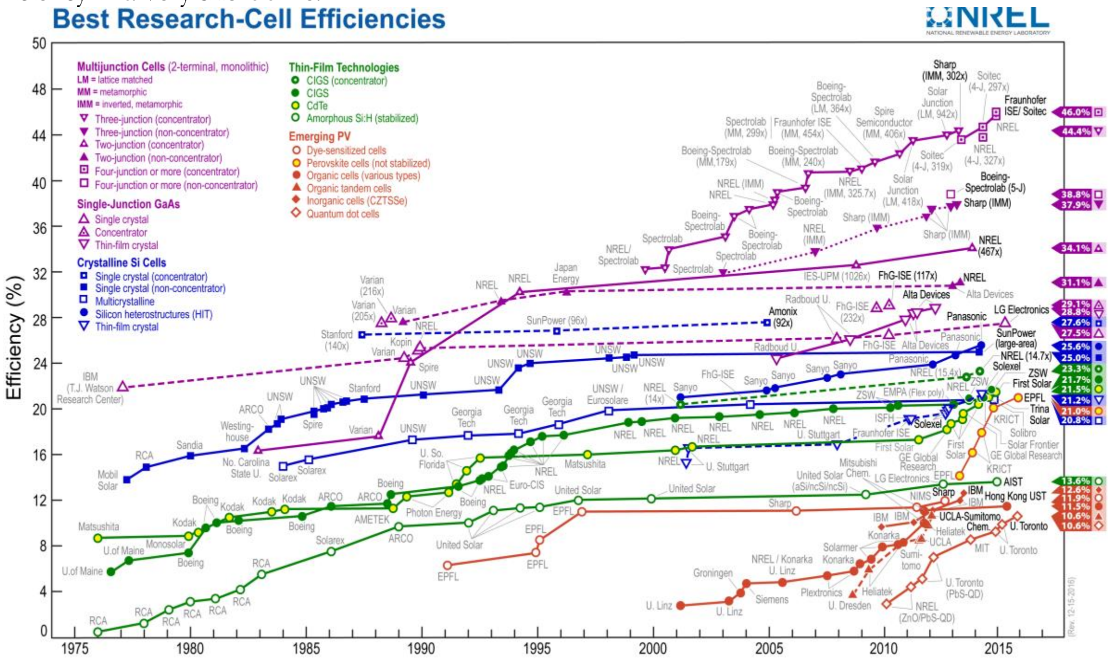

Figure 1. Improvement in photo-electric conversion efficiency of various photovoltaic technologies (NREL) [7]

Hybrid organic-inorganic perovskites absorb light in a manner comparable to silicon-based devices. However, devices based on rigid semiconducting materials require expensive fabrication processes and complex handling techniques. Perovskite devices are flexible, easy to manufacture, and cheaper in price as they are formulated from inexpensive abundant materials. Contrary to this, Si-based devices include expensive fabrication i.e. silicon cutting, high purification, and crystal growth control. Perovskite materials exhibit the dual property of simple & stress-free processing and very high light conversion efficiency. What makes perovskites particularly appealing is their unique combination of simple processing and exceptional light conversion efficiency. From the day of their discovery, they have been successfully incorporated into applications like solar cells, light-emitting diodes (LEDs), lasers, photodetectors, and transistors. A summary of their applications is provided in Figure 2. Perovskite sensitizer ABX_3 (A: CH_3NH_3, B: Pb, Sn, and X: Cl, Br, I) has a number of advantages which include low-cost fabrication and earth abundance along with exciting optical properties mentioned earlier.

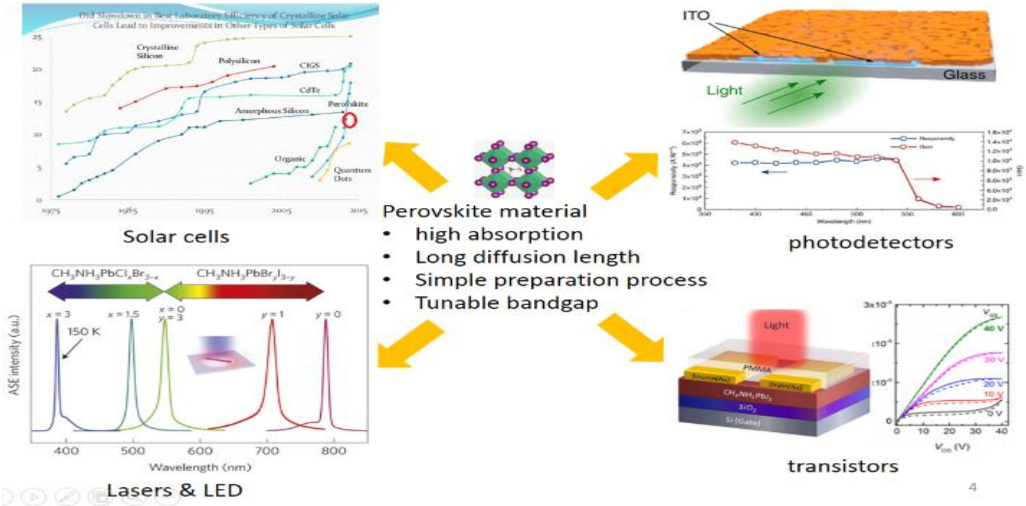

Figure 2. Various applications of perovskite materials as per existing literature

Figure 3 shows the basic perovskite crystal structure schematic for ABX3 in the idealized cubic stage. In a single cubic unit cell, a compound type A is usually present at the corner positions while the type B (metal) atom position is in the center. Type X (halide) components are present at the face centers of the unit cell. This crystal structure stability requirements are very rigid and can be distorted easily. A minor distortion or buckling can lead to less symmetric distorted versions (orthorhombic, tetragonal, etc.). In a less symmetric version, the resting position of A, B, and X and interspacing distance vary.

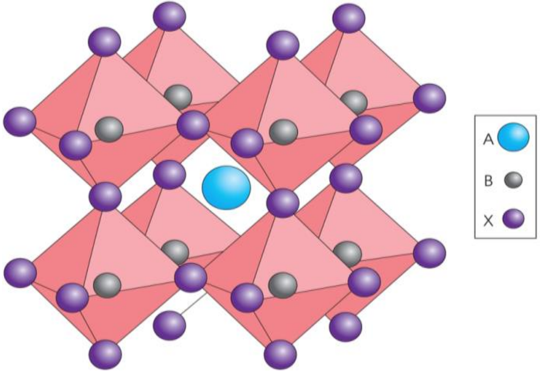

Figure 3. The schematic of the perovskite crystal structure

Therefore, this structure has high tunability as a number of combinations can be made on the same structure and the ones with the better performance can be utilized. Apart from studying behaviors of different perovskite structures, the impact of physical changes on the performance of the whole PSC has also been an area of interest for scientists [8][9]. In this paper, the impact of the physical change in the solar cell i.e. the change in the thickness of the perovskite is observed. It gives the details of the solar cell parameters. It describes the importance and results of Lead halide-based perovskite solar cells and also describes the prominence of Tin halide-based perovskite solar cells.

Objectives:

The main objective of this study is to reach an optimal perovskite layer thickness which provides the best solar cell performance. For this purpose, a novel approach is to compare lead-based and tin-based perovskites. Parameters like efficiency, short circuit current (Jsc), open circuit voltage (Voc), and Fill Factor (FF) are measured for different thickness levels.

Methodology:

Figure 4 describes the methodology flow of this study. In this section, first of all, some of the input parameters like materials, thickness range, band gap, electron affinity, and permittivity were selected. After that, a simulation environment was created to test the performance parameters of perovskite layers. In the last step, the results were compared with previous studies in order to suggest the suitable thickness of perovskite layers. The perovskite solar cell used in this study consisted of five distinct layers, as illustrated in Figure 5.

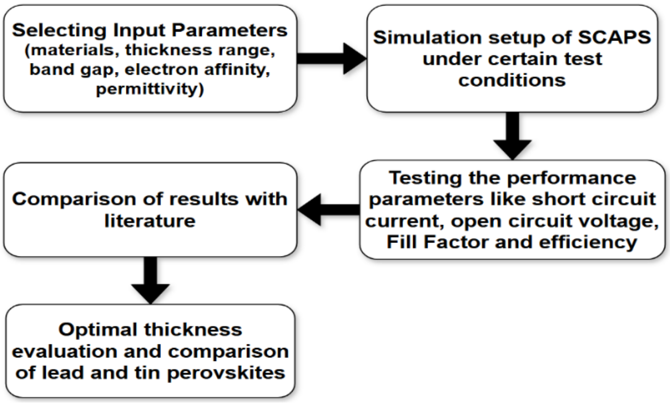

Figure 4. Flow diagram of a methodology

The top contact layer was made of gold (Au), followed by the Hole Transport Layer (HTL) which consisted of Spiro-OMeTAD. The absorber layer was comprised of $CH_3NH_3PbX_3$ or $CH_3NH_3SnX_3$, which served as the core component of the device and was the material of interest in this study. The Electron Transport Layer (ETL), made of TiO_2, was located next to the absorber layer, and the FTO layer was positioned at the bottom.

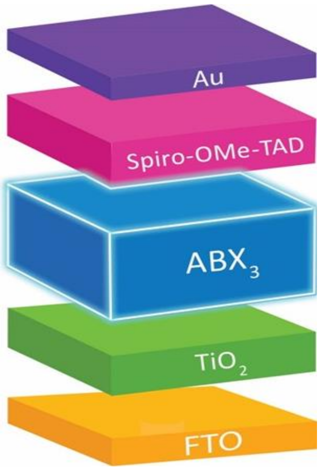

Figure 5. Schematic structure of the perovskite solar cell

Photovoltaic characteristics utilized for device modeling:

To analyze the characteristics of the Perovskite solar cell, the SCAPS-1D simulator was employed. The simulations were carried out under Standard Test Conditions (STC), which were AM 1.5G, 1000 W/m^2, and the temperature of T=300 K. Hole Transport Layer (Spiro-OMe-TAD) was a p-type material. On

On the other hand, the perovskite layer, Electron Transport Layer (TiO_2), and FTO all were n-type materials in the simulations. The parameters utilized in the simulation are outlined in the subsequent section.

Parameters for simulation:

The simulations for all the perovskite materials were done by varying the value of thickness from 0.1 μm to 1 μm. All other parameters were kept constant in each case. The presents the parameters used for simulation [10][11][12][13][14]. Following are some performance parameters mathematical expressions whose trends are discussed in the subsequent section:

The most critical parameters of the solar cell material are its diffusion length and surface passivation. When the surface is perfectly passivized and photon generation is uniform, the equation for the short-circuit current density can be approximated as:

$$Jsc = qG(Ln + Lp) \quad 1$$

Here G is the generation rate, while Ln and Lp are the diffusion lengths of the electron and hole respectively.

$$Jsc \propto G(Ln + Lp) \quad 2$$

Table 1. Parameters of the various layers of the solar cell

Parameters **Materials**	**Thickness (µm)**	**Bandgap (eV)**	**Electron Affinity (eV)**	**Dielectric permittivity**
Spiro-OMeTAD (HTL)	0.5	2.9	2.2	3
$MAPbI_3$	0.1-1.0	1.5	3.93	30
$MAPbBr_3$	0.1-1.0	2.33	3.7	7.5
$MAPbCl_3$	0.1-1.0	2.9	3.293	6.5
$MASnI_3$	0.1-1.0	1.24	4.2	6.5
$MASnBr_3$	0.1-1.0	1.3	4.1	10
TiO_2 (ETL)	0.05	3.26	4.2	10
FTO	0.3	3.5	4	9

Voc is given as here I_L and Io represent photo-generated current and saturation current respectively & T is temperature.

$$Voc = nk\frac{T}{q}\, ln\left(\frac{IL}{I0} + 1\right) \quad 3$$

$$Voc \propto \ln\left(\frac{1}{Io}\right) \quad 4$$

The Fill Factor (FF) in solar cell technology is defined as the maximum power output divided by the product of open circuit voltage (Voc) and short circuit current (Isc) as shown below.

$$FF = \frac{Pmax}{Isc*Voc} = \frac{Impp*Vmpp}{Isc*Voc} \quad 5$$

Solar cell efficiency is the ratio of maximum power output produced by the solar cell to the input power it receives, given as:

$$\eta = \frac{Pout}{Pin} = \frac{Impp*Vmpp}{Pin} = \frac{Isc*Voc*FF}{Pin} \quad 6$$

Organic Lead Halide Based Perovskites:

Lead halide perovskites have emerged as excellent materials for use in photovoltaic and light-emission applications due to their remarkable optoelectronic properties. [7][15][16]. The general formula for lead halides is $APbX_3$, where A can be an inorganic (Cs^+) or organic ($CH(NH_2)^{2+}$, $CH_3NH_3^+$) cation, while X is a halide (I^-, Br^-, or Cl^-). The main reason for the extensive use of lead halides as photovoltaic materials is their exceptional power conversion efficiency (PCE) which is above 22% [17][18]. In addition to their impressive PCE, these semiconducting materials possess many remarkable properties, such as intense photoluminescence, low cost and easy synthesis, high dielectric constants, low excitation binding energies, high absorption coefficients, and long excitation diffusion lengths [19][20].

Furthermore, the perovskite structure offers a high degree of tunability owing to the wide range of available cations (A), central elements, and anions (X). As a result, a multitude of "hybrid" structures can be created and applied in various contexts, offering optical tunability across the whole visible spectrum. This feature has contributed to the growing interest in perovskite materials and their usage potential over an extensive range of applications, from solar cells to light-emitting diodes and beyond [21]

Experimental Setup:

For this study, the cation $CH_3NH_3^+$ and the Metal Pb part were kept constant in the perovskite structure and the performance analysis was done by changing the halide part only. Three halides (I, Br, Cl) were employed for the simulation and the comparison between their performances was done. All the remaining parameters were kept constant. The perovskite layer thickness was increased gradually from 0.1-1 μm. The thickness of all the other layers including the HTL, ETL, and FTO was kept constant. The energy band diagrams of these configurations are shown in Figure 6.

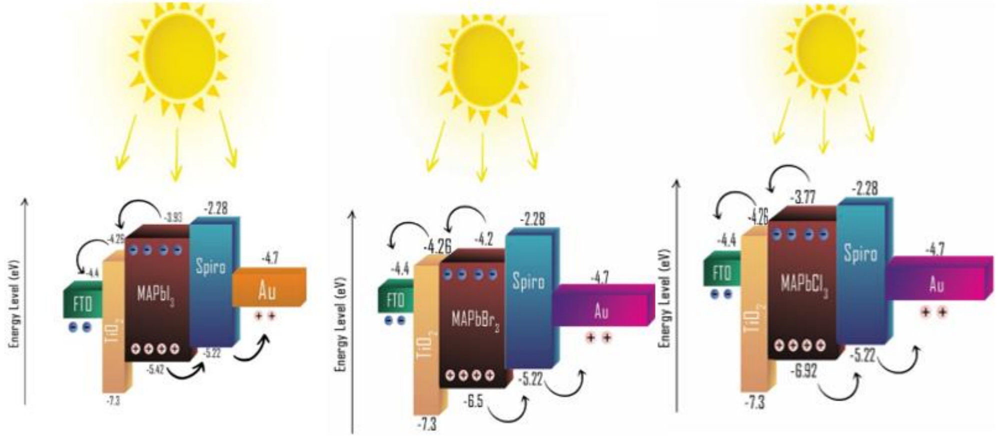

Figure 6. Energy Band diagram using MAPbI3, MAPbBr3 and MAPbCl3 as perovskite layer

Organic Tin Halide based perovskites:

The general formula of Tin halide perovskites is ASnX3, here A can be an inorganic (Cs^+) or organic ($CH_3NH_3^+$) cation, while X is halide (I^-, Br^-, or Cl^-). This perovskite structure is tunable to a great extent because of the option of choosing between various organic or inorganic cations (A) and anions (X), which allows for the formation of different "hybrid" structures. Consequently, tin halide perovskites demonstrate excellent versatility, allowing their integration into a wide range of applications. Organic tin halide-based perovskites have dominated as a competent material to be utilized in solar cells. These materials have several advantages, including high stability, low toxicity, and tunable bandgaps that can be modified to match the solar spectrum. In addition, they have high absorption coefficients and long carrier lifetimes, leading to high photovoltaic performance. The unique optical and electronic properties of organic tin halide perovskites make them a capable alternative to traditional silicon-based solar cells.

Harmful effects of Lead:

Lead has been proven harmful to the human body as well as the environment in several ways as elaborated below:

- Pb-containing compounds can take various routes to enter the bloodstream such as ingestion, inhalation, and dermal contact
- Pb can disrupt the activity of enzymes and receptors upon entering the body, as it mimics the presence of crucial elements like Ca, Zn, and Fe.
- Pb toxicity primarily affects the Central Nervous System (CNS) since it resembles Ca and can easily cross the blood-brain barrier and accumulate in the brain, causing oxidative damage similar to Hg, Cd, and As.
- Lead may accumulate in bones in the form of lead phosphate, whose half-life is 20-30 years, leading to a slow elimination process.
- Chronic exposure to lead can cause neurological disorders, such as cognitive impairment, motor dysfunction, and behavioral issues like depression, anxiety, and aggression.
- When perovskite solar cells degrade in an open environment, they can produce PbI_2, which subsequently breaks down into $Pb(OH)_2$ and HI. The acidic reaction of Hydrogen iodide has more harmful effects than the consumption of $Pb(OH)_2$ [22].

Performance comparison of Tin and Lead in solar cells:

Undoubtedly, lead has proven to be a highly effective element in solar cell absorber layers. Photovoltaic cells utilizing lead halide perovskite absorbers have achieved impressive efficiencies while exhibiting relatively minimal stability concerns. On the other hand, tin-based perovskite PV cells have shown efficiencies of almost 12% so far [23]. Choosing the best material here is actually finding an optimal result having better efficiency, stability as well as user and environment safety.

Experimental setup:

For this study, the metal part Pb was replaced with Sn. The cation $CH_3NH_3^+$ and the Metal Sn part were again kept constant in the perovskite structure and the performance analysis was done by changing the halide part only. The halides that were used for the simulation are I and Br. Cl was excluded from this comparison because of its poor results, especially the worse efficiency obtained. A comparison between the performances was made. All the remaining parameters were kept constant. The perovskite layer thickness was increased gradually from 0.1-1 µm. The thickness of all the other layers including the HTL, ETL, and FTO is kept constant. The energy band diagrams of these configurations are shown in Figure 7.

Figure 7Figure 7. Energy Band diagram using MASnI3 and MASnBr3 as perovskite layer

Results:

The purpose of the simulation was to examine the influence of perovskite layer thickness variation on four key factors of the solar cell, including the J_{SC}, V_{OC}, Fill factor (FF), and overall Efficiency.

Results of MAPbX3 perovskite:

Jsc vs Thickness and Voc vs Thickness trends are shown in Figure 8. It was observed that as the thickness was increased the J_{SC} grew exponentially. The maximum J_{SC} obtained for $MAPbI_3$ is 25.31 mA/cm² at 1µm thickness of the perovskite layer. For $MAPbBr_3$, J_{SC} is 6.92 mA/cm² at 1µm thickness. And for $MAPbCl_3$, J_{SC} is 1.29 mA/cm² at 1µm thickness of the perovskite layer. On the other hand, as the thickness was increased the open circuit voltage (V_{OC}) decreased exponentially. The maximum V_{OC} for $MAPbI_3$ was 2.1 V achieved at 0.1µm thickness of the perovskite layer. For $MAPbBr_3$, VOC was 1.51 V at 0.1µm thickness. For $MAPbCl_3$, VOC was 1.10 V at 0.1µm thickness.

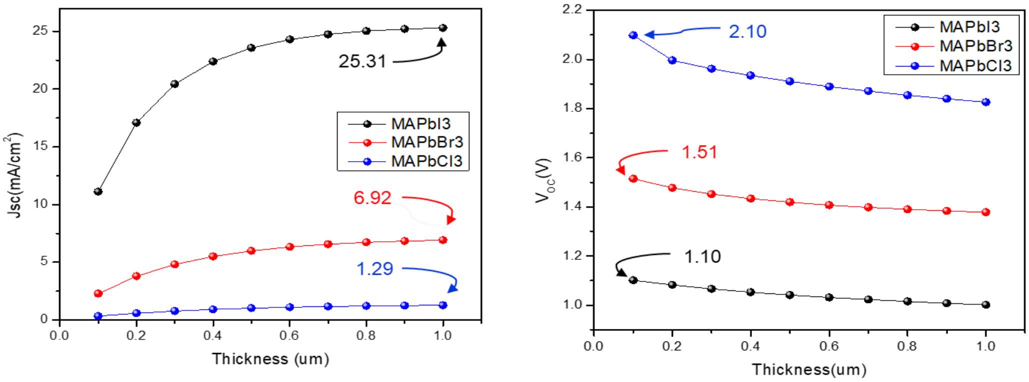

Figure 8. JSC vs Thickness and Voc vs Thickness graph for MAPbX3

FF vs. thickness and Efficiency vs. thickness for MAPbX3 trends are shown in Figure 9. As the thickness was increased FF showed a decreasing trend. The maximum FF for $MAPbI_3$ was 78.72% at 0.1µm thickness of the perovskite layer. For $MAPbBr_3$, the FF was 59.67% at 0.1µm thickness. And for $MAPbCl_3$, the FF was 42.57% at 0.1µm thickness. Finally, for the efficiency, the maximum for $MAPbI_3$ was 15.61% at 0.5µm thickness of the perovskite layer. The maximum efficiency for $MAPbBr_3$ was 4.62% at 0.7µm thickness and the maximum efficiency for $MAPbCl_3$ was 0.83% at 0.9µm thickness.

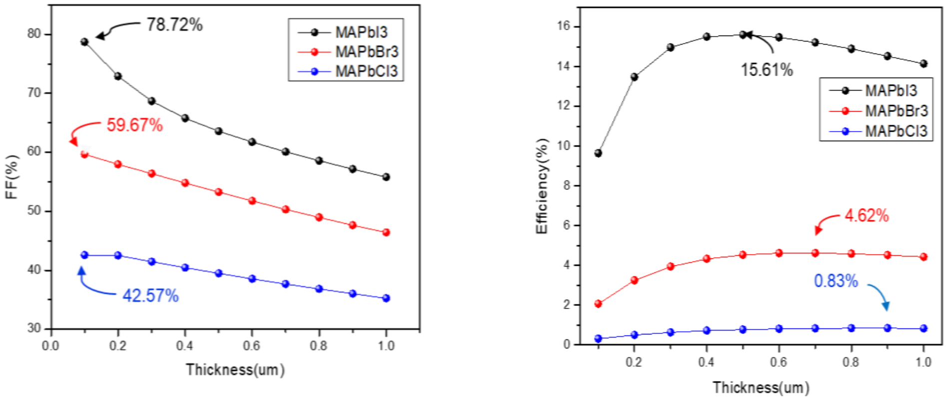

Figure 9. FF Vs Thickness and Efficiency Vs Thickness graph for MAPbX3

Results of MASnX3 perovskite:

Jsc vs Thickness and Voc vs Thickness for MASnX3 trends are shown in Figure 10. As the thickness increased, the short-circuit current density (JSC) showed an exponential rise. The maximum J_{SC} for $MASnI_3$ was 34.65 mA/cm² obtained at 1µm thickness of perovskite layer, while for $MASnBr_3$, J_{SC} was 32.22 mA/cm² at 1µm thickness. For V_{OC}, as the thickness was increased the open circuit voltage (V_{OC}) decreased exponentially. The maximum V_{OC} for $MASnI_3$ was 0.86 V obtained at 0.1µm thickness of the perovskite layer, while for $MASnBr_3$, V_{OC} was 0.88 V at 0.1µm thickness.

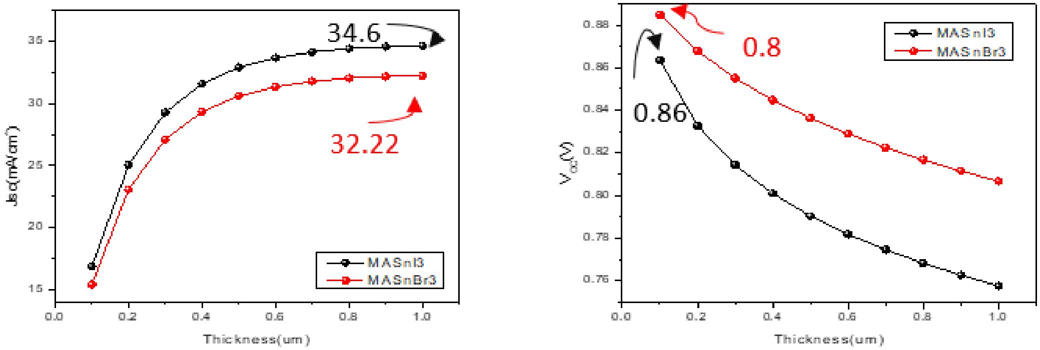

Figure 10. JSC vs Thickness and VOC vs Thickness graph for MASnX3

FF vs Thickness and Efficiency vs Thickness for MASnX3 trends are shown in Figure 11. As the thickness increased, the Fill Factor (FF) exhibited a decreasing trend. The maximum FF for $MASnI_3$ was 80.19 % at 0.1µm thickness of the perovskite layer, while for $MASnBr_3$, the FF was 79.83 % at 0.1µm thickness. Lastly, for efficiency, the maximum for $MASnI_3$ is 18.93 % at 0.5µm thickness of the perovskite layer. On the other hand, the maximum efficiency for $MASnBr_3$ is 19.00 % at 0.5µm thickness.

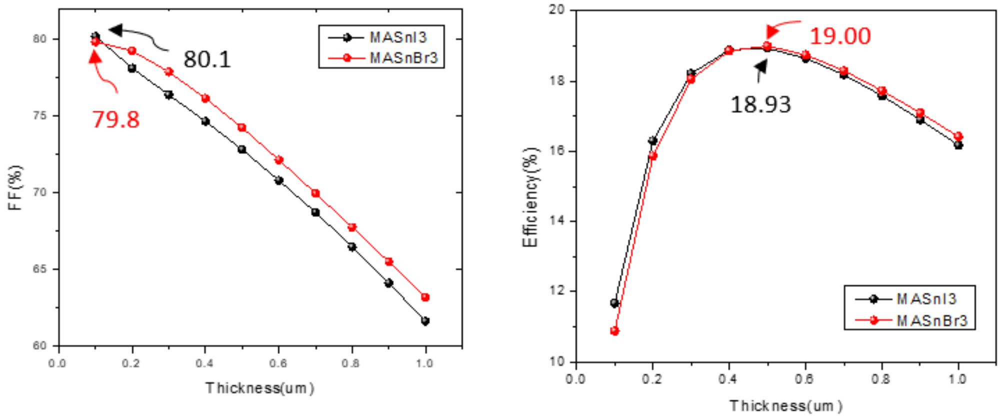

Figure 11. FF vs Thickness and Efficiency vs Thickness graph for MASnX3

Combined results at maximum Efficiency:

The relation of the current density with the voltage at maximum efficiency for both cases is shown in Figure 12.

The results indicate that the highest performance in both cases was achieved when iodide was used as the halide component. The methyl ammonium lead iodide perovskite solar cell showed a maximum efficiency of 15.6% while the methyl ammonium tin iodide perovskite solar cell showed a maximum efficiency of 19%. The performance of tin halide-based perovskite solar cells was found better than lead halide-based perovskite solar cells.

Results Validation:

This study focuses on four key performance parameters of the solar cell: short-circuit current density (JSC), open-circuit voltage (VOC), fill factor (FF), and overall efficiency. It presents a comprehensive mathematical analysis of the trends observed in the simulations for each of these parameters.

According to [24], the JSC of a solar cell is influenced by several factors, including

Solar cell area
The power and spectrum of the incident light
Optical properties of the cell
Minority-carrier collection probability

From Equation 1 and Equation 2, the short-circuit current of a solar cell is directly influenced by the generation rate and the diffusion length, which represents the average distance traveled by an excited carrier before recombining. When the absorber layer thickness is increased, it leads to a higher rate of electron-hole pair generation, which results in a greater current density. However, this increase in current density also leads to a higher concentration of charge carriers in the path. Consequently, this causes an increase in resistance, leading to a decrease in the diffusion length beyond a certain point. Resultantly the short circuit current density begins to decrease. According to [25], the V_{OC} can be defined as the highest potential difference across the external circuit when there is no current flow. The mathematical expression of V_{OC} is given by Equation 3 and Equation 4. When the perovskite layer thickness is increased, it leads to the abundance of free charges, which subsequently leads to a higher recombination rate of charge carriers. As a result, fewer charges end up reaching the hole or electron transport layers at greater thickness. This causes an amplified of the reverse saturation current and subsequently decreases the open circuit voltage. The mathematical expression for the fill factor is given by Equation 5. Increasing the perovskite layer thickness of a solar cell leads to an increase in the series internal resistance of the cell. This increase in resistance results in a rise in power dissipation within the cell and a subsequent reduction in current flow through it. Additionally, as the perovskite layer thickness increases, the voltage across the cell decreases, resulting in the decrement of the fill factor.

The trends of the J_{SC}, V_{OC}, and fill factor (FF) concerning the increasing thickness of the perovskite layer in a solar cell have been discussed. The solar cell efficiency formula is given by Equation 6. Solar cell efficiency increased at the start due to an increased electron-hole pair generation. However, after a certain thickness, the electric field within the cell decreased, while internal power dissipation and charge carrier recombination rates increased, ultimately causing the J_{SC} to saturate and V_{OC} and fill factor to decrease. As a result, the overall efficiency of the solar cell also decreased.

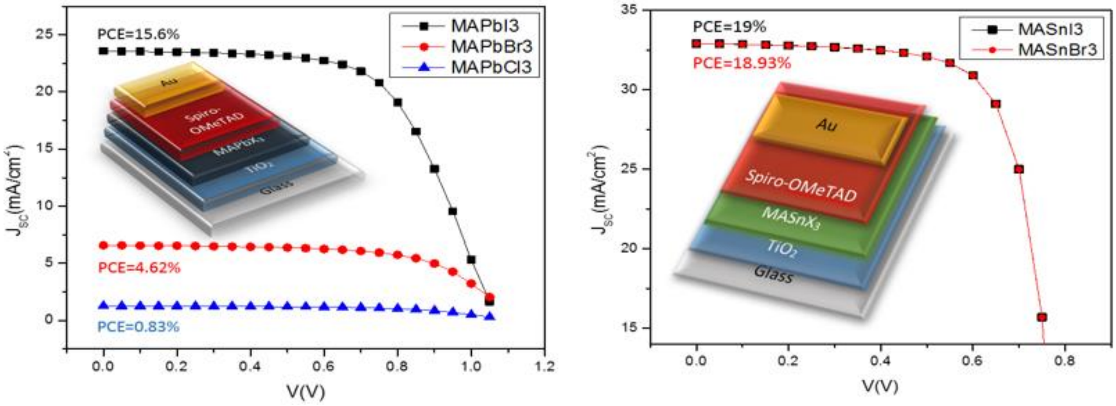

Figure 12. J-V graph of MAPbX3 and MASnX3 at maximum efficiency

Discussion:

Table **1** shows the comparison of both lead-based and tin-based perovskite solar cells Power Conversion Efficiency (PCE) obtained in this proposed work with the previous studies. Lead-based perovskites PCE shows comparable results to previous studies or improved in most cases. However, the tin-based perovskite outperformed previous results and got a huge boost in its PCE making it a strong competitor of lead-based perovskite layers.

Previous research [5] has reported a value as low as 3.9%, whereas this study shows a 15.61% PCE for lead-based $MAPbI_3$. Likewise, this work's simulated $MAPbBr_3$ efficiency was 4.62%, which is in line with the author[7] at 3.8% for that material. Although lead-based perovskites have developed in efficiency, toxicity, and environmental degradation continue to be urgent concerns.

Tin-based perovskite solar cells provide an environment-friendly option to go with. Our simulation of $MASnI_3$ showed a PCE of 18.93%, which is much greater than many experimentally obtained values. The most striking finding of this work was the simulated $MASnBr_3$ performance with a PCE of 19.00%. This is well above the experimental efficiencies reported earlier. Overall, the findings confirm the feasibility of tin-based perovskite photovoltaics as future non-toxic photovoltaic candidates. The simulated high efficiencies prove their hidden potential and merit extensive experimental study to close the gap between theoretical and actual performance.

Table 1. Performance comparison with previous studies

Material	Power Conversion Efficiency (%)	Source
$MAPbI_3$	15.61	Proposed work
	3.9	[5]
$MAPbBr_3$	4.62	Proposed work
	3.8	[7]
$MASnI_3$	18.93	Proposed work
	10.76 ($FASnI_3$)	[23]
	11.22 ($FASnI_3$)	[26]
	14.16	[27]
$MASnBr_3$	19.00	Proposed work
	5.73	[28]

Conclusion:

After the simulation and comparing the results, it is observed that when the thickness of the absorber layer (perovskite layer) in a solar cell increases, it results in the absorption of more photons. This results in the generation of additional electron-hole pairs. This increased absorption leads to an increase in the J_{SC} of the solar cell because more current is generated due to the higher number of charge carriers. However, after a certain thickness, the J_{SC} saturates and then decreases due to the amplified recombination rate of charge carriers and other factors such as reduced electric field and increased series resistance.

The open circuit voltage (V_{OC}) of the solar cell declined with increasing the thickness of the perovskite layer. The reason is the increased recombination of charge carriers, which reduces the number of carriers available for generating voltage. Additionally, as the thickness increases, the reverse saturation current also increases, leading to a further reduction in the open circuit voltage.

The fill factor (FF) decreased when the thickness of the perovskite layer in the solar cell increased. The increment of the perovskite layer thickness leads to an upsurge in the internal resistance of the solar cell, which eventually increases power dissipation in the cell and reduces the current flow in the cell. Additionally, the voltage also decreases on increasing the perovskite layer thickness, further contributing to a decrement in the fill factor. This ultimately resulted in a reduction in the overall efficiency of the solar cell.

The effect of perovskite layer thickness on the efficiency of a solar cell is initially positive, with an increase in efficiency up to a certain point. This is because an increased perovskite layer thickness results in an increased electron-hole pair generation, which leads to an increase in the J_{SC} and therefore an increase in efficiency. However, after a certain thickness, the internal resistance of the solar cell increases, leading to the decrement of fill factor (FF) and an increase in power dissipation, which ultimately causes a drop in efficiency. The decline in efficiency is also due to the increase in charge carrier recombination rates, which causes a reduction in the V_{OC}. Therefore, the primary determinants of the performance of the solar cell in this investigation are the absorption efficiency of the active layer and the rate of movement of the charge carrier towards the appropriate electrode which directly depends on the thickness of the absorber layer.

References:

[1] F. Guo, Z. Xiao, and J. Huang, "Fullerene Photodetectors with a Linear Dynamic Range of 90 dB Enabled by a Cross-Linkable Buffer Layer," *Adv. Opt. Mater.*, vol. 1, no. 4, pp. 289–294, Apr. 2013, doi: 10.1002/ADOM.201200071;PAGE:STRING:ARTICLE/CHAPTER.

[2] G. Xing *et al.*, "Long-range balanced electron-and hole-transport lengths in organic-inorganic CH3NH3PbI3," *Science (80-.).*, vol. 342, no. 6156, pp. 344–347, Oct. 2013, doi: 10.1126/SCIENCE.1243167/SUPPL_FILE/XING.SM.PDF.

[3] S. D. Stranks *et al.*, "Electron-hole diffusion lengths exceeding 1 micrometer in an organometal trihalide perovskite absorber," *Science (80-.).*, vol. 342, no. 6156, pp. 341–

344, Oct. 2013, doi: 10.1126/SCIENCE.1243982/SUPPL_FILE/STRANKS-SM.PDF.

[4] W. Nie *et al.*, "High-efficiency solution-processed perovskite solar cells with millimeter-scale grains," *Science (80-.).*, vol. 347, no. 6221, pp. 522–525, Jan. 2015, doi: 10.1126/SCIENCE.AAA0472/SUPPL_FILE/NIE.SM.PDF.

[5] Q. Dong *et al.*, "Electron-hole diffusion lengths > 175 μm in solution-grown CH3NH3PbI3 single crystals," *Science (80-.).*, vol. 347, no. 6225, pp. 967–970, Feb. 2015, doi: 10.1126/SCIENCE.AAA5760/SUPPL_FILE/PAPV2.PDF.

[6] M. M. Tavakoli *et al.*, "Highly Efficient Flexible Perovskite Solar Cells with Antireflection and Self-Cleaning Nanostructures," *ACS Nano*, vol. 9, no. 10, pp. 10287–10295, Aug. 2015, doi: 10.1021/ACSNANO.5B04284/SUPPL_FILE/NN5B04284_SI_001.PDF.

[7] W. Zhang, G. E. Eperon, and H. J. Snaith, "Metal halide perovskites for energy applications," *Nat. Energy*, vol. 1, no. 6, pp. 1–8, May 2016, doi: 10.1038/NENERGY.2016.48;SUBJMETA=1130,2798,299,301,4077,639,766;KWRD=ELECTRONIC+AND+SPINTRONIC+DEVICES,ENERGY+SCIENCE+AND+TECHNOLOGY,MATERIALS+FOR+ENERGY+AND+CATALYSIS.

[8] A. Husainat, W. Ali, P. Cofie, J. Attia, and J. Fuller, "Simulation and Analysis of Methylammonium Lead Iodide (CH<sub>3</sub>NH<sub>3</sub>PbI<sub>3</sub>) Perovskite Solar Cell with Au Contact Using SCAPS 1D Simulator," *Am. J. Opt. Photonics*, vol. 7, no. 2, p. 33, 2019, doi: 10.11648/J.AJOP.20190702.12.

[9] Q. Chen *et al.*, "Under the spotlight: The organic–inorganic hybrid halide perovskite for optoelectronic applications," *Nano Today*, vol. 10, no. 3, pp. 355–396, Jun. 2015, doi: 10.1016/J.NANTOD.2015.04.009.

[10] M. S. Islam *et al.*, "Defect Study and Modelling of SnX3-Based Perovskite Solar Cells with SCAPS-1D," *Nanomater. 2021, Vol. 11, Page 1218*, vol. 11, no. 5, p. 1218, May 2021, doi: 10.3390/NANO11051218.

[11] Y. Raoui, H. Ez-Zahraouy, N. Tahiri, O. El Bounagui, S. Ahmad, and S. Kazim, "Performance analysis of MAPbI3 based perovskite solar cells employing diverse charge selective contacts: Simulation study," *Sol. Energy*, vol. 193, pp. 948–955, Nov. 2019, doi: 10.1016/J.SOLENER.2019.10.009.

[12] L. Ocaña, C. Montes, S. González-Pérez, B. González-Díaz, and E. Llarena, "Characterization of a New Low Temperature Encapsulation Method with Ethylene-Vinyl Acetate under UV Irradiation for Perovskite Solar Cells," *Appl. Sci. 2022, Vol. 12, Page 5228*, vol. 12, no. 10, p. 5228, May 2022, doi: 10.3390/APP12105228.

[13] S. Tao *et al.*, "Absolute energy level positions in tin- and lead-based halide perovskites," *Nat. Commun. 2019 101*, vol. 10, no. 1, pp. 1–10, Jun. 2019, doi: 10.1038/s41467-019-10468-7.

[14] M. Caputo *et al.*, "Electronic structure of MAPbI3 and MAPbCl3: importance of band alignment," *Sci. Rep.*, vol. 9, no. 1, pp. 1–11, Dec. 2019, doi: 10.1038/S41598-019-50108-0;SUBJMETA=1005,119,299,301,639,766,995;KWRD=CONDENSED-MATTER+PHYSICS,ELECTRONIC+PROPERTIES+AND+MATERIALS,MATERIALS+FOR+DEVICES,MATERIALS+FOR+ENERGY+AND+CATALYSIS.

[15] N. G. Park, M. Grätzel, and T. Miyasaka, "Organic-inorganic halide perovskite photovoltaics: From fundamentals to device architectures," *Org. Halide Perovskite Photovoltaics From Fundam. to Device Archit.*, pp. 1–366, Jan. 2016, doi: 10.1007/978-3-319-35114-8/COVER.

[16] S. A. Veldhuis *et al.*, "Perovskite Materials for Light-Emitting Diodes and Lasers," *Adv. Mater.*, vol. 28, no. 32, pp. 6804–6834, Aug. 2016, doi: 10.1002/ADMA.201600669;REQUESTEDJOURNAL:JOURNAL:15214095;WGROUP:STRING:PUBLICATION.

[17] M. Saliba *et al.*, "Cesium-containing triple cation perovskite solar cells: improved stability, reproducibility and high efficiency," *Energy Environ. Sci.*, vol. 9, no. 6, pp. 1989–1997, Jun.

2016, doi: 10.1039/C5EE03874J.

[18] "Best Research-Cell Efficiency Chart | Photovoltaic Research | NREL." Accessed: Jun. 14, 2025. [Online]. Available: https://www.nrel.gov/pv/cell-efficiency

[19] Q. Lin, A. Armin, P. L. Burn, and P. Meredith, "Organohalide Perovskites for Solar Energy Conversion," *Acc. Chem. Res.*, vol. 49, no. 3, pp. 545–553, Mar. 2016, doi: 10.1021/ACS.ACCOUNTS.5B00483/ASSET/IMAGES/MEDIUM/AR-2015-00483Y_0004.GIF.

[20] D. A. Egger, A. M. Rappe, and L. Kronik, "Hybrid Organic-Inorganic Perovskites on the Move," *Acc. Chem. Res.*, vol. 49, no. 3, pp. 573–581, Mar. 2016, doi: 10.1021/ACS.ACCOUNTS.5B00540/ASSET/IMAGES/LARGE/AR-2015-00540X_0003.JPEG.

[21] M. C. Weidman, M. Seitz, S. D. Stranks, and W. A. Tisdale, "Highly Tunable Colloidal Perovskite Nanoplatelets through Variable Cation, Metal, and Halide Composition," *ACS Nano*, vol. 10, no. 8, pp. 7830–7839, Aug. 2016, doi: 10.1021/ACSNANO.6B03496/SUPPL_FILE/NN6B03496_SI_002.MPG.

[22] G. Schileo and G. Grancini, "Lead or no lead? Availability, toxicity, sustainability and environmental impact of lead-free perovskite solar cells," *J. Mater. Chem. C*, vol. 9, no. 1, pp. 67–76, Jan. 2021, doi: 10.1039/D0TC04552G.

[23] B. Bin Yu *et al.*, "High-efficiency tin perovskite solar cells by the dual functions of reduced voltage loss and crystal regulation," *Mater. Des.*, vol. 228, p. 111850, Apr. 2023, doi: 10.1016/J.MATDES.2023.111850.

[24] "Short-Circuit Current | PVEducation." Accessed: Jun. 14, 2025. [Online]. Available: https://www.pveducation.org/pvcdrom/solar-cell-operation/short-circuit-current

[25] "Solar Cell Parameters equivalent - 9 Solar Cell Parameters and Equivalent Circuit 9 External solar - Studocu." Accessed: Jun. 14, 2025. [Online]. Available: https://www.studocu.com/row/document/institute-of-technology-of-cambodia/solar-energy/solar-cell-parameters-equivalent/80590398

[26] X. Liu *et al.*, "Templated growth of FASnI3 crystals for efficient tin perovskite solar cells," *Energy Environ. Sci.*, vol. 13, no. 9, pp. 2896–2902, Sep. 2020, doi: 10.1039/D0EE01845G.

[27] Z. Zhang, J. Liu, H. Bi, L. Wang, Q. Shen, and S. Hayase, "Over 14% efficiency of highly reproducible Sn perovskite solar cell via defect passivation and morphology repairment," *Chem. Eng. J.*, vol. 483, p. 149345, Mar. 2024, doi: 10.1016/J.CEJ.2024.149345.

[28] F. Hao, C. C. Stoumpos, D. H. Cao, R. P. H. Chang, and M. G. Kanatzidis, "Lead-free solid-state organic–inorganic halide perovskite solar cells," *Nat. Photonics 2014 86*, vol. 8, no. 6, pp. 489–494, May 2014, doi: 10.1038/nphoton.2014.82.